

## Article

# One-Pot Tandem Catalytic Epoxidation—CO<sub>2</sub> Insertion of Monounsaturated Methyl Oleate to the Corresponding Cyclic Organic Carbonate

Roberto Calmanti , Nicola Sargentoni, Maurizio Selva  and Alvisè Perosa \* 

Dipartimento di Scienze Molecolari e Nanosistemi, Università Ca' Foscari Venezia, Via Torino 155, 30172 Venezia Mestre, Italy; roberto.calmanti@unive.it (R.C.); 877616@stud.unive.it (N.S.); selva@unive.it (M.S.)

\* Correspondence: alvisè@unive.it

**Abstract:** Conversion of unsaturated fatty acids, FAMES or triglycerides into the corresponding cyclic organic carbonates involves two reaction steps—double-bond epoxidation and CO<sub>2</sub> insertion into the epoxide—that are generally conducted separately. We describe an assisted-tandem catalytic protocol able to carry out carbonation of unsaturated methyl oleate in one-pot without isolating the epoxide intermediate. Methyl oleate carbonate was obtained in 99% yield and high retention of *cis*-configuration starting from methyl oleate using hydrogen peroxide and CO<sub>2</sub> as green reagents, in a biphasic system and in the presence of an ammonium tungstate ionic liquid catalyst with KBr as co-catalyst.

**Keywords:** direct oxidative carboxylation; tandem catalysis; cyclic organic carbonates; tungstate ionic liquids



**Citation:** Calmanti, R.; Sargentoni, N.; Selva, M.; Perosa, A. One-Pot Tandem Catalytic Epoxidation—CO<sub>2</sub> Insertion of Monounsaturated Methyl Oleate to the Corresponding Cyclic Organic Carbonate. *Catalysts* **2021**, *11*, 1477. <https://doi.org/10.3390/catal11121477>

Academic Editor: Claudia Carlucci

Received: 2 November 2021

Accepted: 24 November 2021

Published: 2 December 2021

**Publisher's Note:** MDPI stays neutral with regard to jurisdictional claims in published maps and institutional affiliations.



**Copyright:** © 2021 by the authors. Licensee MDPI, Basel, Switzerland. This article is an open access article distributed under the terms and conditions of the Creative Commons Attribution (CC BY) license (<https://creativecommons.org/licenses/by/4.0/>).

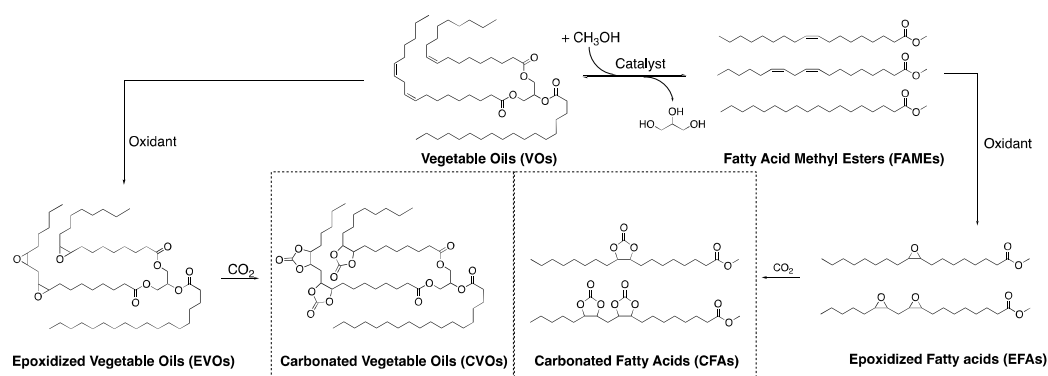
## 1. Introduction

Ever-increasing attention has been focused in recent decades on the synthesis of cyclic organic carbonates (COCs) from carbon dioxide. Although recent studies suggest that only less than 1% of CO<sub>2</sub> generated from anthropogenic emissions can be effectively recycled into chemicals [1,2] and that other trapping strategies are needed to reduce excess CO<sub>2</sub>, nonetheless the preparation of COCs via the catalytic activation of CO<sub>2</sub> remains one of the most efficient strategies in green organic synthesis for its exploitation as a C1 building block and for its fixation into stable organic products and/or polymers [3]. This is even truer when renewable bio-based feedstocks such as glycerol, carbohydrates, terpenes and vegetable oils (VOs) are used [4]. The latter class, in particular, is interesting for multiple reasons which include the large commercial availability of VOs up to 200 MT per year [5], the relatively easy transesterification of vegetable oils into their components as fatty acids methyl esters (FAMES) through the biodiesel manufacture, and the use of VOs as intermediates for a plethora of chemical compounds [6]. In this respect, the conversion of VOs and FAMES to the corresponding carbonates is traditionally described as illustrated in Scheme 1.

The protocol shown is a two-step procedure comprised of an initial epoxidation reaction to obtain the corresponding epoxidized vegetable oils (EVOs, left) or epoxidized fatty acids (EFAs, right), followed by the subsequent insertion of CO<sub>2</sub> to achieve either carbonated vegetable oils (CVOs, center left) or carbonated fatty acids (CFAs, center right). These compounds find applications as lubricants [7], plasticizers for PVC [8], and building blocks for the synthesis of non-isocyanate polyurethanes (NIPUs) [9].

The first step (epoxidation) is a well-established reaction conducted in the presence of different oxidants (H<sub>2</sub>O<sub>2</sub>, organic peroxides, organic peracids) and both homogeneous and heterogeneous catalysts such as, for example, polyoxometalates or lipases. This subject has been accurately reviewed elsewhere [10]. Although the production of epoxidized

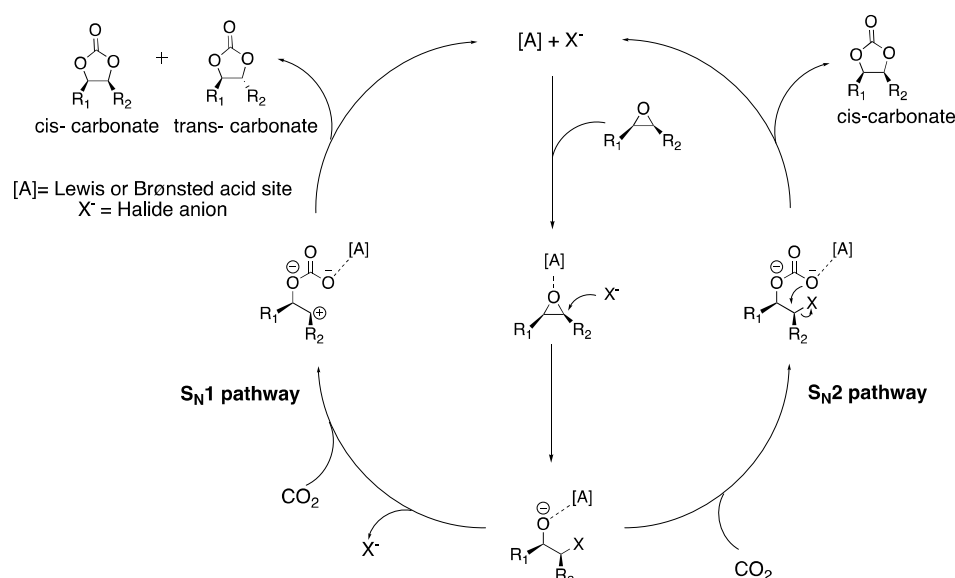
fatty acids (EFAs) is not yet available on a commercial scale, epoxidized vegetable oils (EVOs) are currently produced in industry by the Prilazahev procedure which is a conventional epoxidation process carried out with strong oxidants such as peracetic acid or performic acid and strong mineral acids as catalysts [11]. This method, however, suffers from several drawbacks including: (i) low epoxidation chemoselectivity due to oxirane ring opening; (ii) acid corrosion; (iii) safety issues because of the reaction exothermicity ( $\Delta H = -55 \text{ kcal}\cdot\text{mol}^{-1}$  per each carbon–carbon double bond) [12]; (iv) time consuming and costly isolation and purification of EVOs; (v) formation of non-recyclable waste from exhausted acid catalysts.



**Scheme 1.** Route for the synthesis of carbonated vegetable oils (VOs) and fatty acids methyl esters (FAMES). The case of oleic acid triglyceride and methyl oleate is reported as an example.

The second reaction of Scheme 1, the CO<sub>2</sub> insertion into epoxides, has been proposed with the use of bifunctional catalytic systems such as tetraalkylammonium halides comprised of a Lewis or Brønsted acid site able to electrophilically activate the reactant epoxide and a nucleophilic halide that favors the opening of the epoxide ring. Both experimental data and computational calculations have elucidated the reaction mechanism for terminal epoxides [13], while less clear is the case of internal epoxides such as those of EVOs and EFAs, that are generally available in the stereochemically pure *cis*-configuration. In particular, the stereoselectivity control of the process is not obvious since starting from a pure *cis*-epoxide, both *cis*- and *trans*-carbonate products are achieved whose relative proportions depend on the nature of halide anion of the catalyst (Scheme 2). The better the leaving group ability of the anion (I<sup>−</sup> and to a lesser extent Br<sup>−</sup>) the higher the formation of *trans*-carbonate as the thermodynamically favored product plausibly formed via a S<sub>N</sub>1 mechanism [14]. On the contrary, the use of a poorer leaving groups (Cl<sup>−</sup>) steers the reaction to the exclusive formation of the *cis*-carbonate through a S<sub>N</sub>2 pathway. A role for metal Lewis acid catalysts has been identified in orientating the chemoselectivity towards the *cis*-carbonate products [15]. In this respect, several investigations have also highlighted the effects of the boundary conditions, specifically the cation/halide interactions in the catalysts and the presence of hydrogen bond [16] donors, in altering not only the catalytic activity, but the *cis*/*trans* product distribution [17,18].

Overall, notwithstanding the use of renewable feedstocks as starting substrates, the process of Scheme 1 can be hardly considered under a sustainable chemistry perspective: epoxides, whether they are fossil- or bio- based, are toxic, if not mutagenic, and their synthesis is problematic from both environmental and safety standpoints [19,20]. The obvious conclusion is that in a truly sustainable future, the production, isolation, and handling of epoxidized compounds should be avoided.



**Scheme 2.** Mechanistic pathways for the formation of cyclic organic carbonate via CO<sub>2</sub> fixation into cis-epoxides.

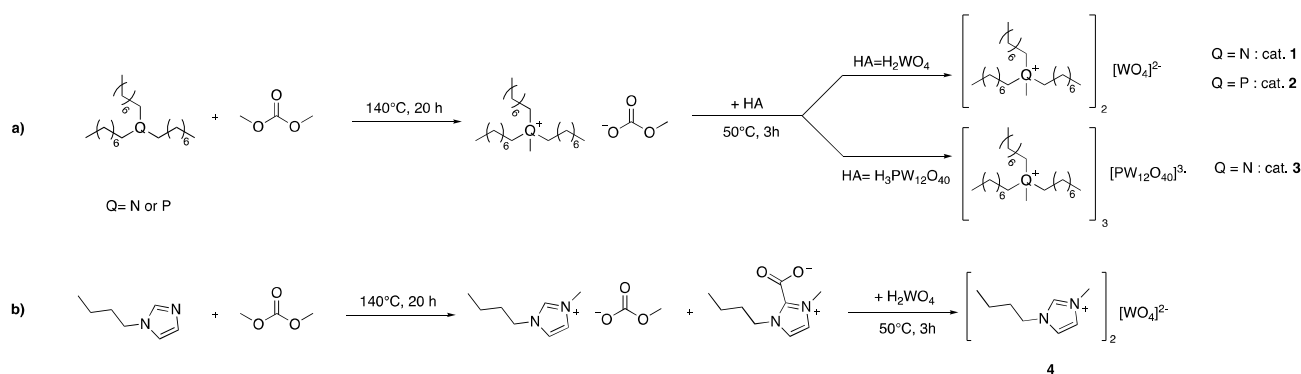
This has been the objective of the present work which was conceived to exploit the chemistry shown in Scheme 1, but with the design of new catalysts by which a tandem sequence—from unsaturated oils as reactants to cyclic carbonates as final products—could be achieved without the need of isolating the epoxide intermediates. This strategy has been very recently reviewed by our group; moreover, according to a new one-pot protocol (auto-tandem catalysis), we demonstrated that several terminal aliphatic and aromatic olefins (11 examples) could be converted into the corresponding carbonates with up to a 95% yield, in the presence of H<sub>2</sub>O<sub>2</sub> as a benign oxidant, a novel [N<sub>8,8,8,1</sub>]<sub>2</sub>[WO<sub>4</sub>] tungstate-based ionic liquid catalyst, [N<sub>4,4,4,4</sub>]I as a nucleophilic co-catalyst, and CO<sub>2</sub> at atmospheric pressure [21,22].

We report here for the first time that the tandem route was successfully extended to internal olefins, in particular methyl oleate (MO) which was chosen as a bio-based model alkene. A series of tungstate-based ionic liquid catalysts were synthesized and tested in combination with simple alkali halide salts co-catalysts. The one-pot procedure was optimized to reach a quantitative conversion of MO with an excellent 99% chemoselectivity towards the desired carbonate product (in a 92:8 cis:trans ratio).

## 2. Results and Discussions

### 2.1. Synthesis of Tungstate-Based Ionic Liquids

A procedure developed by our research group was employed for the synthesis of the tungstate ionic liquid catalysts (TILCs) trioctyl methyl ammonium tungstate ([N<sub>8,8,8,1</sub>]<sub>2</sub>WO<sub>4</sub>, **1**) trioctylmethyl phosphonium tungstate ([P<sub>8,8,8,1</sub>]<sub>2</sub>WO<sub>4</sub>, **2**), and trioctylmethyl ammonium phosphotungstate ([N<sub>8,8,8,1</sub>]<sub>3</sub> PW<sub>12</sub>O<sub>40</sub>, **3**) [21]. The synthetic route is shown in Scheme 3a and the procedures are reported in the experimental part. This methodology does not require any organohalides for the quaternarization of trioctylamine and trioctylphosphine in the first step because dimethyl carbonate (DMC) serves both as methylation agent and as counterion once the quaternarization occurs by forming the -onium methylcarbonate ionic liquids. The second step is a simple acid-base reaction in which a Brønsted acid HA (HA = H<sub>2</sub>WO<sub>4</sub>, HPW<sub>12</sub>O<sub>40</sub>) yields the tungstate-based ionic liquid, the driving force being the irreversible formation of methylcarbonic acid (i.e., the half ester of carbonic acid) that spontaneously decomposed to methanol and CO<sub>2</sub> [23].



**Scheme 3.** Synthesis of tungstate ionic liquid catalysts (TILCs). Path (a) regards the synthesis of trioctylmethylammonium tungstate (**1**), trioctylmethylphosphonium tungstate (**2**) and trioctylmethyl ammonium phosphotungstate (**3**); Path (b) regards the synthesis of butylmethylimidazolium tungstate (**4**).

A similar protocol was applied also for the synthesis of butyl methyl imidazolium tungstate (**4**, Scheme 3b) however the reaction between 1-butylimidazole and DMC resulted in the formation of two main products: 1-butyl-3-methylimidazolium methyl carbonate (the predicted onium salt) and 1-butyl-3-methylimidazolium-2-carboxylate zwitterion in approximately a 2.5/1 ratio as determined by <sup>1</sup>H-NMR spectroscopy (Figure S5) [24]. Once the methylation had occurred, the highly nucleophilic imidazolium C<sub>2</sub> carbon was able to attack the carboxyl carbon of DMC, hence forming the carboxylate zwitterion by the elimination of methanol. The mixture of ionic liquid and zwitterion was concentrated under vacuum to achieve a 97% isolated mixture and the <sup>1</sup>H-NMR and <sup>13</sup>C-NMR spectra are reported in the supporting information (Figures S5 and S6). The mixture, upon addition of tungstic acid yielded the desired 1-butyl-3-methyl-imidazolium tungstate (BMIM<sub>2</sub>WO<sub>4</sub>, **4**) ionic liquid, as a single product in nearly quantitative yield (95%).

The ionic liquids **1–4** were fully spectroscopically characterized by <sup>1</sup>H-NMR, <sup>13</sup>C-NMR, <sup>31</sup>P-NMR, <sup>183</sup>W-NMR, FT-IR and the spectra are reported in Figures S7–S24.

All the TILCs **1–4** showed the IR bands associated with the cations, in particular the -CH<sub>2</sub> symmetric and asymmetric and the -CH<sub>3</sub> stretching between 2850 and 3000 cm<sup>-1</sup>. **1** and **3** showed the band associated to the N-CH<sub>3</sub> stretching between 1200 and 1100 cm<sup>-1</sup>, while **2** showed three characteristic peaks associated to the P-CH<sub>3</sub> asymmetric deformation at 1466 cm<sup>-1</sup>, the P-CH<sub>3</sub> symmetric deformation at 1378 cm<sup>-1</sup> and the P-CH<sub>3</sub> rocking at 977 cm<sup>-1</sup>. The presence of the tungstate ion was confirmed by the adsorption associated to the W-O bond. For the tetrahedral WO<sub>4</sub><sup>2-</sup> anion, two active modes were observed at about 927 and 825 cm<sup>-1</sup>, respectively symmetric and asymmetric stretching [25].

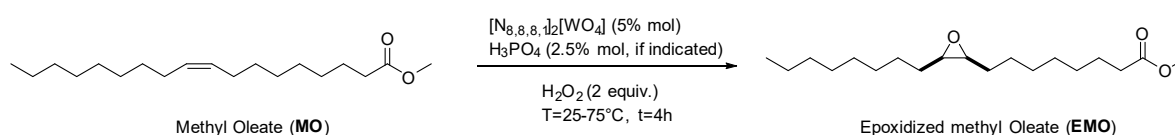
The <sup>1</sup>H- and <sup>13</sup>C-NMR spectra of all the TILCs **1–4** confirmed the disappearance of the peaks associated methyl carbonate anion, while the <sup>31</sup>P-NMR spectrum of **2** and **3** showed the presence of a single peak, indicating the presence of a single species for the phosphonium cation and the phosphotungstate anion.

Comparison of the <sup>1</sup>H-NMR spectrum of [BMIM]<sub>2</sub>(WO<sub>4</sub>) (Figure S21) with its precursors (Figure S5) was indicative of the formation of **4**. The chemical shifts of the three imidazolium protons H<sub>2</sub>, H<sub>4</sub>, H<sub>5</sub> of [BMIM]<sub>2</sub>(WO<sub>4</sub>) indicated different hydrogen-bonding and confirmed stronger H-bonding between cation and anion in [BMIM]<sub>2</sub>(WO<sub>4</sub>) as already reported by us in a previous work [26]. Furthermore, the H<sub>2</sub> chemical shift integrated less than unity, indicating that this proton was largely engaged in H-bonding with WO<sub>4</sub><sup>2-</sup>, in agreement with the higher basicity of the WO<sub>4</sub><sup>2-</sup> anion compared to the methyl carbonate one.

Finally, the <sup>183</sup>W-NMR spectra of the TILCs **1**, **2** and **4** were diagnostic of the presence of monomeric tungstate [WO<sub>4</sub>]<sup>2-</sup> as a single resonance was observed in the range +10–-10 ppm, different respect to the sodium tungstate reference [27]. The <sup>183</sup>W-NMR spectrum of **3** showed a single resonance at -85 ppm as already reported in the literature [28].

## 2.2. Epoxidation of Methyl Oleate

The epoxidation of methyl oleate (MO) to epoxidized methyl oleate (EMO) (Scheme 4) was conducted in a two-phase system by using  $\text{H}_2\text{O}_2$  as oxidant.  $[\text{N}_{8,8,8,1}]_2(\text{WO}_4)$  (**1**) was chosen as the model TILC to first investigate the reaction parameters and phosphoric acid ( $\text{H}_3\text{PO}_4$ ) was chosen as co-catalyst due to its ability to boost the activity of tungstate-based catalysts by forming in-situ phosphonate-di(peroxo)tungstate species [21,29]. The results are reported in Figure 1.



**Scheme 4.** Epoxidation of methyl oleate (MO) to epoxidized methyl oleate (EMO).

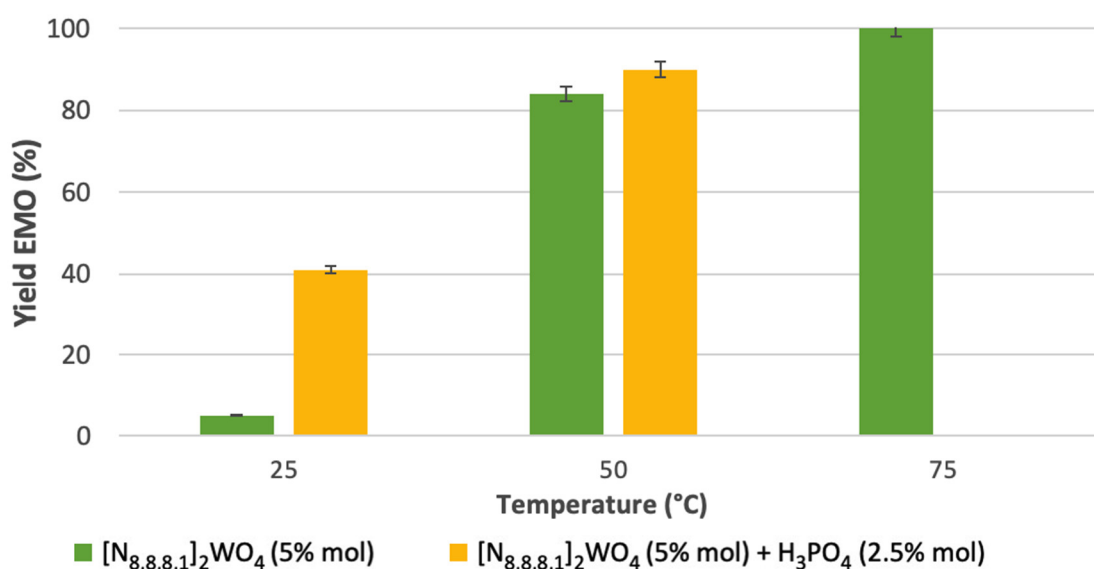


**Figure 1.** Epoxidation of methyl oleate (MO, 1.69 mmol) in the presence of  $\text{H}_2\text{O}_2$  (2 equivalent) at  $T = 25\text{--}75^\circ\text{C}$  for 4 h with only  $[\text{N}_{8,8,8,1}]_2(\text{WO}_4)$  as catalyst (green bars) and with the addition of  $\text{H}_3\text{PO}_4$  as co-catalyst (yellow bars). Yields calculated by  $^1\text{H}$  NMR (nuclear magnetic resonance) spectroscopy using mesitylene as internal standard. Chemoselectivity towards epoxidized methyl oleate (EMO) is always quantitative.

The epoxidation performed at  $25^\circ\text{C}$  showed a great difference of reactivity if the reaction is conducted in the presence of the TILC solely (green bars) with respect to the addition of  $\text{H}_3\text{PO}_4$  as co-catalyst (yellow bars): 5 and 41% yield for EMO were obtained respectively. This difference was less evident when the reaction was carried out at higher temperature ( $T = 50^\circ\text{C}$ ) where the EMO yields were 84% and 90%, respectively. This prompted us to increase the temperature to  $75^\circ\text{C}$  in the co-catalyst-free reaction; a quantitative conversion of MO with a complete chemoselectivity to EMO was obtained. This effect was in contrast with what we found out in our previous publication for terminal olefins for which the use of a P-based promoter was compulsory to reach high yields in the epoxide [21]: this is probably due to the higher reactivity of disubstituted internal olefins respect to terminal ones towards epoxidation [30]. Since the use of a simplified procedure that excludes the use of auxiliaries is beneficial from a green perspective, we pursued our investigation without the addition of  $\text{H}_3\text{PO}_4$  as co-catalyst. In this case, the peroxotungstate species are the only ones accountable for the epoxidation of the substrate. As expected, the reaction mechanism led to the selective formation of the cis-epoxide [31]. Finally, a blank test conducted at  $75^\circ\text{C}$  for 4 h in the absence of any catalyst confirmed a lack of conversion in these conditions.

The effect of oxidant amount ( $\text{H}_2\text{O}_2 = 1\text{--}4$  equivalent respect to the substrate MO) was subsequently studied with two different amounts of catalyst (2.5–5% mol) and the results

reported in Figure 2. With 2.5% mol catalyst (orange bars) conversion is never quantitative: an increase of the yields is observed going from 1 to 4 equivalents of  $\text{H}_2\text{O}_2$ , reaching a maximum yield of 86%. On the other hand, the use of 5% mol of  $[\text{N}_{8,8,8,1}]_2[\text{WO}_4]$  with an equimolar amount of  $\text{H}_2\text{O}_2$  afforded a 41% yield, while the use of 2 equivalent  $\text{H}_2\text{O}_2$  allowed to reach quantitative conversion of MO and complete chemoselectivity to EMO [32]. In these experimental conditions,  $\text{H}_2\text{O}_2$  titration test showed the complete disappearance of hydrogen peroxide after the completion of the reaction ( $75^\circ\text{C}$ , 4 h). This suggested an overall 50% efficiency of hydrogen. Unexpectedly, a larger excess of hydrogen peroxide (3 and 4 equivalent) affected the biphasic system and led to lower conversion probably due to the formation of different, less-active peroxy-tungstate species, as already reported elsewhere [32–34]. Moreover, a large excess of hydrogen peroxide can be detrimental for the subsequent  $\text{O}_2$  fixation step in the tandem process, as already stated in our previous work.

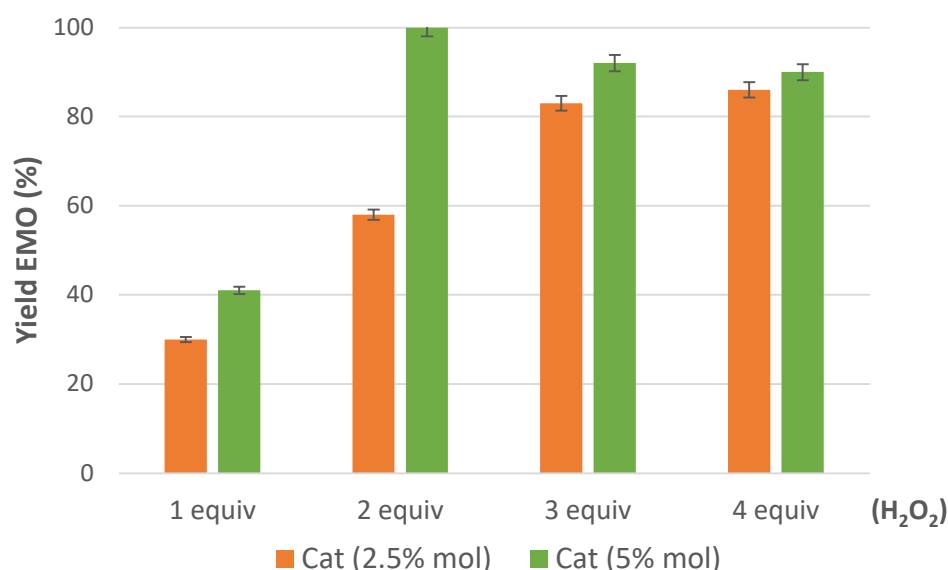


**Figure 2.** Epoxidation of methyl oleate (1.69 mmol) with different amount of  $\text{H}_2\text{O}_2$  (30% *w/w*, 1–4 equivalent) at  $T = 75^\circ\text{C}$ ,  $t = 4$  h in presence of  $[\text{N}_{8,8,8,1}]_2[\text{WO}_4]$  (Cat = 2.5–5% mol) as catalyst. Yields calculated by  $^1\text{H}$  NMR spectroscopy using mesitylene as internal standard. Chemoselectivity towards EMO is always quantitative.

The optimized results obtained using  $[\text{N}_{8,8,8,1}]_2[\text{WO}_4]$  (**1**) and the other TILCs (**2–4**) are reported in Figure 3. While **1** achieved a quantitative conversion of MO and chemoselectivity towards EMO, all the other TILCs showed lower catalytic activity toward the epoxidation. The second-best catalyst,  $[\text{P}_{8,8,8,1}]_2(\text{WO}_4)$  **2**, reached only 69% conversion to MO. While quaternary ammonium salts are widely studied for the epoxidation of FAMES [10,31,35], in contrast quaternary phosphonium salts were only recently described [36] and evidence highlighted the possible formation of the phosphine oxide from the phosphonium cation [37,38]. The different catalytic activity is likely due to the physical properties of **1** and **2** [39] and the coulombic interactions between organic cation and tungstate anion which modulate the physical and chemical activity of the TILCs [40]. A recent study proposed a tunability of ionic liquid systems in which electronic environments, i.e. chemical properties, are tuned via the anion and physical properties are tuned via the cation [39].

$[\text{N}_{8,8,8,1}]_3(\text{PW}_{12}\text{O}_{40})$  (**3**) was insoluble both in water as well as in methyl oleate and thus required the use of dichloromethane as solvent. Only 11% conversion was observed. Finally,  $[\text{BMIM}]_2(\text{WO}_4)$  (**4**) showed no catalytic activity at all, probably because  $[\text{BMIM}]_2(\text{WO}_4)$  partitions in the aqueous phase and thus is unable to transfer the active peroxotungstate species to the organic phase.

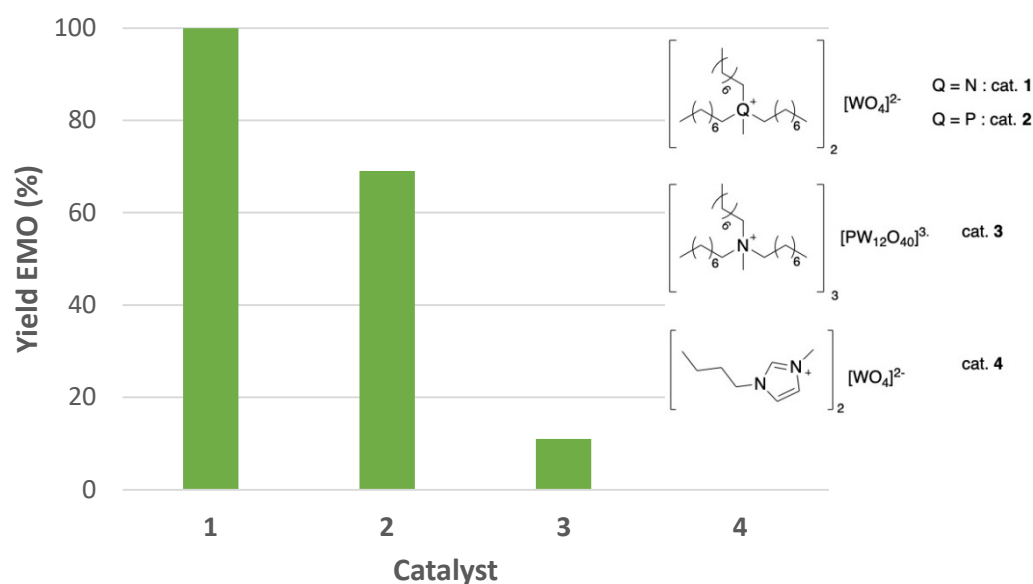


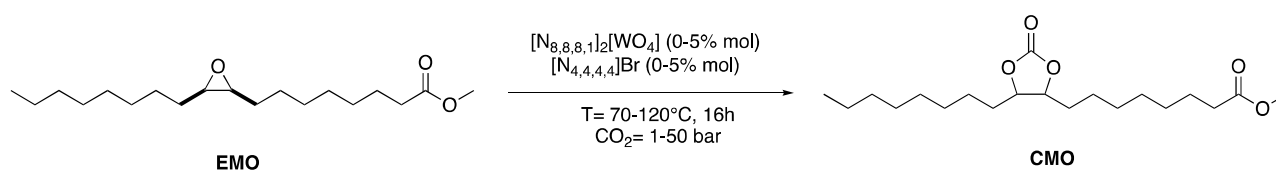
**Figure 3.** Reaction conditions: methyl oleate (1.69 mmol),  $\text{H}_2\text{O}_2$  (30% w/w, 2 equivalent), tungstate catalyst (5% mol),  $T = 75^\circ\text{C}$ ,  $t = 4\text{ h}$ , solvent-free. Conversion and yield calculated by  $^1\text{H}$  NMR spectroscopy using mesitylene as internal standard. Chemoselectivity towards EMO is always quantitative.

Finally, a 10-fold increase of the starting material showed that our system was scalable and a 95% isolated yield of epoxidized methyl oleate (4.82 g, 15.42 mmol, >97% purity according to GC analysis and  $^1\text{H}$  NMR spectroscopy) was obtained with the optimized procedure which involves the reaction of MO (5.021 g, 16.93 mmol) with  $\text{H}_2\text{O}_2$  (3.46 mL, 30.88 mmol) and  $[\text{N}_{8,8,8,1}]_2(\text{WO}_4)$  (0.759 g, 0.77 mmol), in a 1:2:0.05 molar ratio, at  $75^\circ\text{C}$  for 4 h. At the end of the reaction, the mixture was filtered through silica in order to remove the catalyst. The mixture was then extracted with dichloromethane, dried over sodium sulfate and filtered. The organic phase was collected and concentrated under vacuum to achieve the pure product. The conversion of MO was quantitative with complete retention of stereochemistry: only *cis* epoxide (*cis*-EMO) was obtained.

The pure epoxidized methyl oleate (EMO) was exploited as starting material to investigate the  $\text{CO}_2$  fixation process.

### 2.3. $\text{CO}_2$ Insertion Step

$\text{CO}_2$  insertion into EMO (Scheme 5) was explored in the presence of the sole  $[\text{N}_{8,8,8,1}]_2[\text{WO}_4]$  (5% mol) as catalyst, with only  $[\text{N}_{4,4,4,4}]\text{Br}$  (1.25–5% mol), or with a mixture of the two at different temperature and pressure of  $\text{CO}_2$ . Results are reported in Table 1. Initially,  $100^\circ\text{C}$ , 50 bar of  $\text{CO}_2$  and 16 h of reaction were chosen as experimental conditions based on previous similar work reported in the literature for EFAs [8,14,41].  $[\text{N}_{8,8,8,1}]_2[\text{WO}_4]$  proved to be active for  $\text{CO}_2$  fixation but only a 28% conversion and 64% chemoselectivity towards the corresponding CMO was observed (entry 1, Table 1). This outcome was similar to that reported by us for the  $\text{CO}_2$  insertion into styrene oxide and terminal olefins with  $[\text{N}_{4,4,4,4}]_2\text{WO}_4$  demonstrating that TILCs are active in the  $\text{CO}_2$  fixation but do not promote complete chemoselectivity towards the desired COC [26]. Epoxide isomerization by-products were observed deriving from the Meinwald rearrangement of the epoxide to the corresponding ketones, as already reported in the literature [42,43].

Scheme 5. CO<sub>2</sub> insertion into EMO.Table 1. CO<sub>2</sub> fixation into epoxidized methyl oleate.

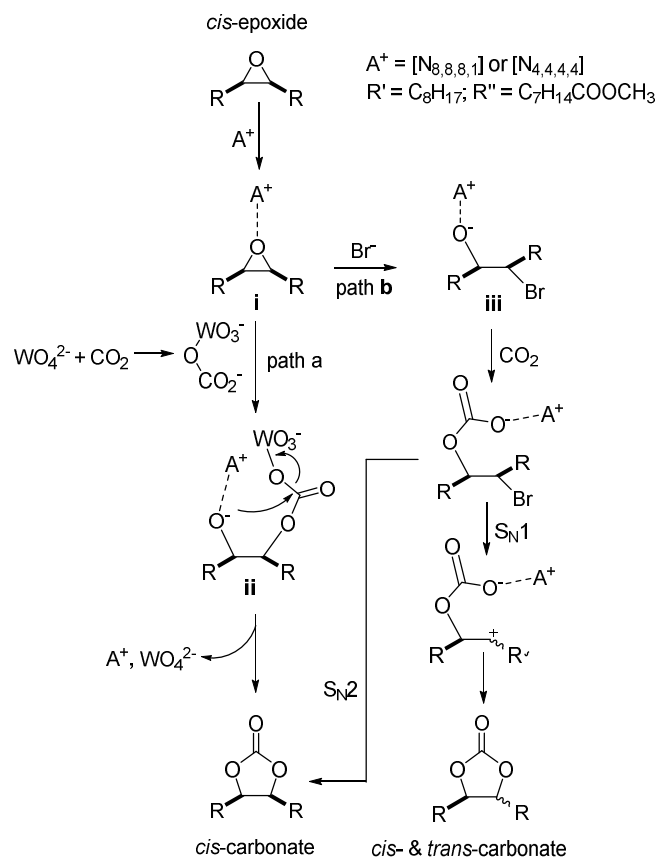
Entry	$p(CO_2)$ Bar	T (°C)	$(N_{8,8,8,1})_2-WO_4$ (% mol)	$[N_{4,4,4,4}]Br$ (% mol)	Conversion EMO	Selectivity CMO	Cis:Trans CMO Ratio
1	50	100	5	-	28	64	99:1
2	50	100		2.5	80	91	56:44
3	50	100	5	2.5	87	94	99:1
4	1	100	5	2.5	7	20	99:1
5	10	100	5	2.5	59	77	90:10
6	50	70	5	2.5	10	100	99:1
7	50	120	5	2.5	50	50	70:30
8	50	100	5	1.25	79	87	99:1
9	50	100	5	5	94	95	99:1
10 <sup>a</sup>	50	100	5	5	47	100	90:10
11 <sup>a</sup>	50	100	-	5	0	0	-

Reaction conditions: EMO (1.60 mmol),  $[N_{8,8,8,1}]_2[WO_4]$  (0–5% mol),  $[N_{4,4,4,4}]Br$  (0–5% mol),  $CO_2 = 1-50$  bar, T = 70–120 °C, 16 h. Conversion, chemoselectivity and cis:trans ratio calculated according to <sup>1</sup>H NMR spectroscopy by using mesitylene as internal standard. <sup>a</sup> NaBr (5% mol) was used in the place of  $[N_{4,4,4,4}]Br$  as halide co-catalyst.

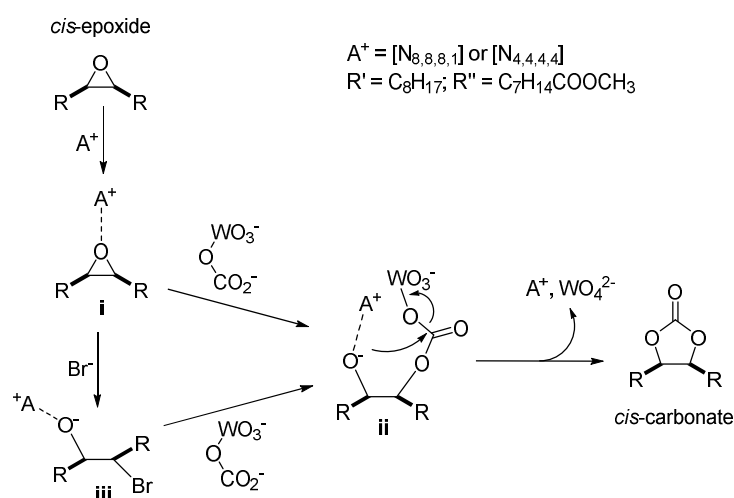
$[N_{4,4,4,4}]Br$  was likewise active for CO<sub>2</sub> insertion but was also unable to afford complete conversion and chemoselectivity towards the carbonate of methyl oleate (80% and 91%, respectively, entry 2, Table 1) and, most importantly, the reaction afforded a 56:44 *cis:trans* mixture of stereoisomers as observed by <sup>1</sup>H-NMR spectroscopy. The independent roles of  $[N_{8,8,8,1}]_2[WO_4]$  and  $[N_{4,4,4,4}]Br$  in promoting CO<sub>2</sub> insertion were rationalized by the mechanisms of Scheme 6. In both cases, the first step is the activation of the methyl oleate epoxide by a Lewis acidic species such as the ammonium moiety forming intermediate (i). With only trioctylmethylammonium tungstate, CO<sub>2</sub> insertion follows path a, (Scheme 6) and involves the formation of an active  $[WO_4 \cdot CO_2]^{2-}$  adduct as indicated by <sup>183</sup>W-NMR spectroscopy (Figure S25) and already reported in the literature [44]. This pathway leads to direct insertion of CO<sub>2</sub> on the same face of the methyl oleate epoxide oxygen with formation of intermediate (ii) locked in the indicated configuration by the electrostatic interaction between tungstate and the ammonium moiety A<sup>+</sup>, this ring-closes to give the *cis*-carbonate. Pathway b with only tetrabutylammonium bromide, involves ring-opening of the methyl oleate epoxide by S<sub>N</sub>2 attack of the bromide on the opposite face respect to the methyl oleate epoxide oxygen with inversion of configuration and formation of the alkoxide (iii). The mechanism then follows the established pathway involving the alkoxide attacking CO<sub>2</sub> followed by carbonate ring-closure either by an S<sub>N</sub>2 or S<sub>N</sub>1 pathway. S<sub>N</sub>1 leads to loss of stereoselectivity and formation of a mixture of *cis*- and *trans*-methyl oleate carbonate.

The concurrent presence of both  $[N_{8,8,8,1}]_2[WO_4]$  and  $[N_{4,4,4,4}]Br$  was much more efficient compared to when  $[N_{4,4,4,4}]Br$  was used alone: it prompted 87% conversion of the *cis*- methyl oleate epoxide with 94% chemoselectivity towards the carbonate of methyl oleate and a 99:1 *cis:trans* stereoselectivity (entry 3, Table 1). To explain the synergic tungstate-bromide effect, we propose that the active  $[WO_4 \cdot CO_2]^{2-}$  adduct can either insert directly into the activated epoxide (i) or react by S<sub>N</sub>2 on the bromo-alkoxide (iii), thereby generating the same stereocontrolled intermediate (ii) as in path a of Scheme 6, which

immediately ring-closes to yield the methyl oleate *cis*-carbonate (Scheme 7). This increased *cis*-selectivity was already observed by Leitner et al. in the synthesis of cyclic carbonates from oleochemical epoxides and CO<sub>2</sub> in the presence of ammonium halide and transition metal substituted silicotungstate polyoxometalates [16].



**Scheme 6.** Pathways for insertion of CO<sub>2</sub> into internal *cis*-epoxides in the presence of [N<sub>8,8,8,1</sub>]<sub>2</sub>[WO<sub>4</sub>] (path a) or [N<sub>4,4,4,4</sub>]Br (path b).



**Scheme 7.** Pathways for insertion of CO<sub>2</sub> into internal *cis*-epoxides in the concurrent presence of both [N<sub>8,8,8,1</sub>]<sub>2</sub>[WO<sub>4</sub>] and [N<sub>4,4,4,4</sub>]Br.

The effect of CO<sub>2</sub> pressure, temperature, co-catalyst amount and ammonium halide (entries 4–10, Table 2) were investigated in view of optimizing conversion and selectivity.

**Table 2.** Assisted direct oxidative carboxylation of methyl oleate.

Entry	Co-Catalyst (5% mol)	Product Distribution <sup>a,b</sup>			CMO Cis:Trans Ratio
		EMO (%)	CMO (%)	By-Products <sup>c</sup> (%)	
1 <sup>d</sup>	[N <sub>4,4,4,4</sub> ]Br	67	33	0	99:1
2	[N <sub>4,4,4,4</sub> ]Cl	80	20	0	99:1
3	[N <sub>4,4,4,4</sub> ]Br	55	45	0	99:1
4	[N <sub>4,4,4,4</sub> ]I	35	65	0	90:10
5	NaCl	78	22	0	99:1
6	NaBr	54	46	0	99:1
7	NaI	23	67	10	56:44
8	KCl	77	23	0	99:1
9	KBr	30	70	0	95:5
10	KI	35	65	0	96:4
11 <sup>e</sup>	NaBr	46	38	16	93:7
12 <sup>e</sup>	NaI	20	62	18	42:58
13 <sup>e</sup>	KBr	1	99	0	92:8
14 <sup>e</sup>	KI	7	87	6	67:34

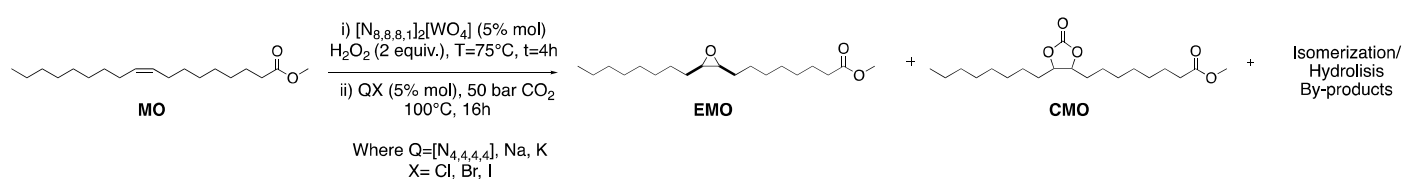
Reaction conditions: Methyl oleate (**MO**, 6.74 mmol), H<sub>2</sub>O<sub>2</sub> (2 equivalent), [N<sub>8,8,8,1</sub>]<sub>2</sub>WO<sub>4</sub> (5% mol) performed at 75 °C for 4 h followed by the addition of a selected co-catalyst (Q<sup>+</sup>X<sup>-</sup> (5% mol), where Q<sup>+</sup> = [N<sub>4,4,4,4</sub>], Na, K; X<sup>-</sup> = Cl<sup>-</sup>, Br<sup>-</sup>, I<sup>-</sup>) was added to the reaction mixture, the reactor was sealed and placed in an autoclave with 50 bar of CO<sub>2</sub>. This second step was conducted for 16 h at 100 °C. <sup>a</sup> Conversion of **MO** is always quantitative; <sup>b</sup> Conversion, product distribution and cis:trans ratio calculated by NMR spectroscopy using mesitylene as internal standard; <sup>c</sup> the main by-products are dihydroxy methyl oleate and the corresponding ketones due to Meinwald rearrangement; <sup>d</sup> 2.5% mol of co-catalyst; <sup>e</sup> reaction conducted for 48 h.

Pressures lower than 50 bar CO<sub>2</sub> were insufficient to obtain good yields in CMO. In fact, with 1 bar of CO<sub>2</sub> (entry 4), conversion was only 7% with concurrent formation of over-oxidation byproducts. The main by-products were the corresponding ketones (methyl 9-oxooctadecanoate and methyl 10-oxooctadecanoate) and diol (methyl 9,10-dihydroxyoctadecanoate) according to GC-MS analysis. With 10 bars, CO<sub>2</sub> limited conversion and chemoselectivity were obtained (59% and 77%, respectively, entries 5 and 3) and other experiments (not reported) showed that pressures in the range 20–40 bar were also insufficient. 100 °C was the optimal temperature for the synthesis of CMO: lower temperature (70 °C, entry 6) promoted 100% CMO chemoselectivity but poor conversion (10%); while higher temperature (120 °C, entry 7) lowered conversion as well as chemoselectivity towards CMO. 2.5% mol of [N<sub>4,4,4,4</sub>]Br afforded the best compromise in terms of conversion and chemoselectivity: decreasing it to 1.25% mol led to slightly lower conversion and chemoselectivity towards CMO (from 87% and 94% down to 79 and 87% respectively, entries 3 and 8), while doubling it to 5% mol led to conversion and chemoselectivity (94 and 95% respectively, entry 9) comparable to the reaction with 2.5% mol. No effect on the *cis:trans* ratio was observed.

Finally, substitution of [N<sub>4,4,4,4</sub>]Br with NaBr was explored (entry 10). Albeit with lower conversion (47%), excellent chemo- and stereo-selectivity were achieved, demonstrating that [N<sub>8,8,8,1</sub>]<sub>2</sub>[WO<sub>4</sub>] can play a dual role: on the one hand it acts as phase-transfer agent for NaBr, on the other it activates CO<sub>2</sub> towards the insertion into the epoxide. As expected, NaBr was inactive in the absence of [N<sub>8,8,8,1</sub>]<sub>2</sub>[WO<sub>4</sub>] (entry 11).

#### 2.4. Tandem Reaction

Having established the optimal conditions for each of the two separate epoxidation and CO<sub>2</sub> insertion steps, the direct tandem process for oxidative carboxylation of methyl oleate was explored (Scheme 8).



**Scheme 8.** Direct tandem oxidative carboxylation of methyl oleate.

An auto-tandem protocol with all the reagents present from the onset was initially tested. Unfortunately, no reaction was observed when methyl oleate (2 g, 6.76 mmol),  $\text{H}_2\text{O}_2$  (30% *v/v*, 2 equivalent),  $[\text{N}_{8,8,8,1}]_2[\text{WO}_4]$  (5% mol) and  $[\text{N}_{4,4,4,4}](\text{Br})$  (2.5% mol) were combined and pressurized with 50 bar of  $\text{CO}_2$  and heated at  $100^\circ\text{C}$  for 16 h. This lack of reactivity was probably due to the reaction between  $[\text{N}_{4,4,4,4}]\text{Br}$  and the oxidant which are in fact often exploited simultaneously for the bromination of various organic substrates [45,46].

An assisted-tandem approach where the bromide co-catalyst is added after the epoxidation step was, therefore, implemented. Experiments on the assisted-DOC of methyl oleate are reported in Table 2. In the first experiment, methyl oleate (6.76 mmol) and  $\text{H}_2\text{O}_2$  (2 equivalent) were added in a glass reactor in the presence of  $[\text{N}_{8,8,8,1}]_2\text{WO}_4$  (5% mol) and stirred at  $75^\circ\text{C}$  for 4 h. Then,  $[\text{N}_{4,4,4,4}](\text{Br})$  (2.5% mol, entry 1) was added to the reaction mixture and the reactor was placed in an autoclave with 50 bar of  $\text{CO}_2$  for 16 h at  $100^\circ\text{C}$ . Quantitative conversion was observed and a 33% yield of CMO was obtained.

The amount of co-catalyst was increased to 5% mol and tetrabutylammonium chloride, bromide and iodide were explored for comparison (entries 1–3): complete conversion but limited chemoselectivity towards CMO (20–65%, entry 1–3, Table 2) were observed in all cases albeit with formation of the *cis*-carbonate (99:1 for chloride and bromide, 90:10 for iodide) confirming the beneficial role of tungsten in the epoxidation step also in controlling stereoselectivity. The low chemoselectivity towards CMO is probably caused by the presence of the biphasic system that decreases the rate of the  $\text{CO}_2$  fixation reaction compared to the tests reported above for  $\text{CO}_2$  insertion in the solventless system (see entries 2 and 3, Table 1 and entry 2, Table 2 for comparison).

To overcome the conversion limitations, alkali (Na and K) halides were tested (entries 5–10) in place of the ammonium counterparts. This class of compounds is not active for  $\text{CO}_2$  insertion into epoxides unless in the presence of cryptands [47,48], or of a phase-transfer agent as shown above. Alkali halides present in the aqueous  $\text{H}_2\text{O}_2$  phase could therefore become active for  $\text{CO}_2$  insertion in the presence of  $[\text{N}_{8,8,8,1}]_2\text{WO}_4$ . NaCl (entry 5) and NaBr (entry 6) were tested and the assisted-tandem DOC of methyl oleate yielded 100% conversion and 22% and 46% yields of CMO, respectively, with complete stereospecificity towards the *cis*- isomer. NaI (entry 7) led to 100% conversion but lower 67% chemoselectivity towards CMO due to the formation of overoxidation by-products and poor stereoselectivity (56:44 *cis*:*trans*) indicative of the competitive  $\text{S}_{\text{N}}1$  pathway of intermediate **ii** of Scheme 6, likely due to the better leaving group ability of iodide. By using potassium halides KBr (entry 9) and KI (entry 10), 70% and 65% CMO yields were observed (entries 8 and 9, respectively) with a *cis*:*trans* ratio > 95:5.

In summary, CMO yields obtained with the sodium halides (entries 5–7, 22, 46% and 67% respectively) were virtually identical to those obtained with the corresponding tetraalkylammonium salts (entries 1–3: 20, 45% and 65% respectively) and the product distribution was in agreement with the reported trend for the  $\text{CO}_2$  insertion in water ( $\text{Cl}^- < \text{Br}^- < \text{I}^-$ ) [17,49].

It should be stressed that the assisted-tandem process, albeit slower than the  $\text{CO}_2$  insertion experiments reported in Table 1, prompted the exclusive formation of EMO and CMO (except with NaI) while the tests performed on the single  $\text{CO}_2$  fixation step showed formation of the corresponding diol and ketones derived from isomerization (compare Tables 1 and 2). One can conclude that the biphasic mixture favors chemoselective formation of the cyclic organic carbonate of methyl oleate. To date, this is the first example of direct oxidative carboxylation of an oleochemical such as methyl oleate.

Having verified that alkali bromide and iodide salts function for the CO<sub>2</sub> insertion step, attention was focused on improving the performance of the reaction and thus the yield of carbonate. A series of reactions was run over a period of 48 h with NaBr, NaI, KBr and KI (entries 11–14, Table 2).

Curiously, the chemoselectivity towards CMO after 48 h dropped compared to 4 h, both with NaBr (entries 6 and 11, from 46 to 38%) as well as with NaI (entries 7 and 12, from 67% to 62%): this was probably due to the formation of side products (i.e., the corresponding diol, ketone and perhaps polymerization products) related to the longer reaction at 100 °C. A very different outcome was observed by using KBr (entry 13) and KI (entry 14): with KBr, an excellent 99% yield of CMO was achieved after 48 h (entry 13) with high stereoselectivity (*cis:trans* = 92:8) while the use of KI led to an 87% yield of CMO accompanied by the minor formation of the above-mentioned by-products and with moderate stereoselectivity (*cis:trans* = 67:34).

Since the tungstate catalyst is likely to remain in its active form at the end of the process, recovery and reuse of the catalytic system was explored, but unfortunately remains an unresolved issue. The recovery and reuse of the catalytic system was explored but remains an unresolved issue. Attempts to recover [N<sub>8,8,8,1</sub>]<sub>2</sub>WO<sub>4</sub> by extracting with organic solvents have so far proved to be ineffective due to the partial miscibility of the ionic liquid in both the aqueous and organic phases.

### 3. Conclusions

In summary, we have developed and optimized an assisted-tandem protocol for the direct conversion of an unsaturated fatty acid methyl-ester into its corresponding cyclic organic carbonate. The procedure involves one-pot epoxidation of the double bond of methyl oleate followed by insertion of CO<sub>2</sub>, yielding selectively methyl oleate carbonate. The product was obtained in 99% yield with high retention of *cis*- configuration using hydrogen peroxide and CO<sub>2</sub> as green reagents, in a biphasic system and in the presence of an ammonium tungstate ionic liquid catalyst and KBr as co-catalyst. The main novelty is that the intermediate epoxide does not need to be isolated as was required until now, reducing hazards associated with its handling. In addition, the tungstate ammonium ionic liquid has a crucial multifunctional role in the tandem reaction: in the first step, it promotes epoxidation of the olefin in the biphasic mixture by activating hydrogen peroxide; in the second step, it activates CO<sub>2</sub> for insertion into the epoxide while at the same time controlling the stereochemistry with exclusive formation of the *cis*-carbonate and serving as phase transfer catalyst enabling the use of a simple and economic alkali halide as co-catalyst for the epoxide ring opening. This multifaceted catalytic activity represents a clear innovation in the use of tungsten-based catalysis but also in the synthesis of cyclic organic carbonates.

The added significance of this work lies in having demonstrated and implemented a green, safe and direct protocol that can find potential applications in the upgrading of many classes of unsaturated bio-based platform chemicals including for example triglycerides and their derivatives, as well as terpenes and terpenoids, by converting them into the corresponding cyclic organic carbonates utilizing a green oxidant and green carbon source. The resulting compounds find applications as lubricants, plasticizers, and polymer building blocks.

### 4. Materials and Methods

#### 4.1. General Reagents

Triethylamine (N<sub>8,8,8</sub>), trioctylphosphine (P<sub>8,8,8</sub>), 1-butylimidazole (Blm), dimethyl carbonate (DMC), Tetrabutylammonium chloride (N<sub>4,4,4,4</sub>Cl), Tetrabutylammonium bromide (N<sub>4,4,4,4</sub>Br), tetrabutylammonium iodide (N<sub>4,4,4,4</sub>I), sodium chloride (NaCl), sodium bromide (NaBr), sodium iodide (NaI), potassium bromide (KBr), potassium iodide (KI), methanol (MeOH), diethyl ether (Et<sub>2</sub>O), dichloromethane (CH<sub>2</sub>Cl<sub>2</sub>), oleic acid (OA) were purchased from Sigma-Aldrich/Merck (Milan, Italy). All reagents were ACS grade, and if

not otherwise specified, were employed without further purification. Water was of milli-Q grade. Methyl Oleate (**MO**) was synthesized according to a literature procedure.

#### 4.2. Analyses

GC/MS (EI, 70 eV, Agilent Technologies, Santa Clara, CA, USA) analyses were run using a HP5-MS capillary column (L = 30 m,  $\varnothing$  = 0.32 mm, film = 0.25  $\mu$ m) purchased from Agilent Technologies, (Santa Clara, CA, USA). The following conditions were used. Carrier gas: He; flow rate: 1.2 mL/min; split ratio: 10:1; initial T: 100 °C (2 min), ramp rate: 20 °C/min; final T: 300 °C. NMR spectra were recorded on a NMR spectrometer (Bruker Corporation, Billerica, MA, USA) working at 400 MHz for  $^1\text{H}$ -NMR, 100 MHz for  $^{13}\text{C}$ -NMR, 162MHz for  $^{31}\text{P}$ -NMR and 16 MHz for  $^{183}\text{W}$ -NMR. Chemical shifts were reported in  $\delta$  values downfield from TMS; deuterated chloroform, dimethyl sulfoxide-d6 and oxide deuterium were used as deuterated solvents.

#### 4.3. Synthesis of Catalysts

Methylcarbonate -onium ionic liquids ( $[\text{N}_{8,8,8,1}](\text{CH}_3\text{OCOO})$ ,  $[\text{P}_{8,8,8,1}](\text{CH}_3\text{OCOO})$ ,  $[\text{BMIM}](\text{CH}_3\text{OCOO})$ ) and tungstate ionic liquids ( $[\text{N}_{8,8,8,1}]_2\text{WO}_4$ ,  $[\text{P}_{8,8,8,1}]_2\text{WO}_4$ ,  $[\text{BMIM}]_2\text{WO}_4$ ) were prepared by adjusting methods previously reported by our research groups [21,23].

#### 4.4. Syntheses of Ionic Liquids with Dimethyl Carbonate (DMC)

In a typical procedure,  $\text{N}_{8,8,8}$  (20 mL, 45.2 mmol), DMC (30 mL, 356 mmol) and methanol (20 mL) were combined in a 200 mL stainless steel autoclave fitted with a pressure gauge and a thermocouple for temperature control. Three vacuum- $\text{N}_2$  cycles were applied. The autoclave was heated for 20 h at 140 °C with magnetic stirring (1000 rpm). Then the autoclave was allowed to cool and vented. Methanol and residual DMC were removed from the mixture by rotary evaporation to give  $[\text{N}_{8,8,8,1}](\text{CH}_3\text{OCOO})$  (19.18 g, 95%).

The same procedure was adopted to synthesize both  $[\text{P}_{8,8,8,1}](\text{CH}_3\text{OCOO})$  and  $[\text{BMIm}](\text{CH}_3\text{OCOO})$ .  $^1\text{H}$ -NMR and  $^{13}\text{C}$ -NMR spectroscopy of this last compound proved that  $[\text{BMIm}](\text{CH}_3\text{OCOO})$  was not pure, but the reaction gave a mixture of the predicted ionic liquid, 1-butyl-3-methylimidazolium methyl carbonate, and the zwitterion obtained from the reaction of BIM with DMC, 1-butyl-3-methylimidazolium-2-carboxylate  $[\text{BMIm}^+\text{COO}^-]$  in a 7:3 ratio. This compound was used "as is" without further purification for the synthesis of butylmethylimidazolium tungstate.

All the methylcarbonate -onium ionic liquids were characterized by  $^1\text{H}$ -NMR and  $^{13}\text{C}$ -NMR spectroscopy (Figures S1–S6).

#### 4.5. Syntheses of Tungstate-Based Ionic Liquids (TILCs)

In a conventional procedure,  $\text{H}_2\text{WO}_4$  (3.45 g, 13.80 mmol, 0.6 equivalent) or phosphotungstic acid (5.22 g, 1.81 mmol, 0.6 equivalent) was slowly added to an aqueous solution of  $[\text{Q}](\text{CH}_3\text{OCOO})$  (1 equivalent, where  $\text{Q} = \text{N}_{8,8,8,1}$ ,  $\text{P}_{8,8,8,1}$ ,  $\text{BMIm}$ ) heated at 50 °C.  $\text{H}_2\text{WO}_4$  was added in a slight excess respect to the stoichiometry of the reaction in order to force the complete disappearance of  $[\text{Q}](\text{CH}_3\text{OCOO})$ . The solution was stirred for 3 h during which time the initial opalescent solution turned yellow. The solution was then cooled and extracted three times with ethyl acetate and dried on sodium sulfate. The solution was then filtered, and the ionic liquid was concentrated under vacuum. TILCs were obtained with high yields:  $[\text{N}_{8,8,8,1}]_2(\text{WO}_4)$  (**1**) (9.45 g, yield = 85%);  $[\text{P}_{8,8,8,1}]_2\text{WO}_4$  (**2**) (11.36 g, yield = 97%);  $[\text{N}_{8,8,8,1}]_3(\text{PW}_{12}\text{O}_{40})$  (5.98 g, yield = 97%);  $[\text{BMIm}]_2\text{WO}_4$  (**4**) (5.73 g, yield = 95%).

The tungstate-based ionic liquids were fully characterized by  $^1\text{H}$ -NMR,  $^{13}\text{C}$ -NMR,  $^{31}\text{P}$ -NMR (when necessary),  $^{183}\text{W}$ -NMR and FT-IR spectroscopy. Spectra are reported in the supporting information (Figures S7–S24).

#### 4.6. Reaction Procedures

##### 4.6.1. Synthesis of Methyl Oleate

In a typical procedure, a 250 mL round-bottomed flask equipped with a condenser was charged with oleic acid (20,032 g, 71 mmol) and a large excess methanol (100 mL, 247 mmol). The solution was pre-heated at 50 °C, then concentrated H<sub>2</sub>SO<sub>4</sub> (95%) was added dropwise until a light white solution was formed. The reaction was then performed under reflux with magnetic stirring (1100 rpm) for 4 h. The solution was allowed to cool at room temperature. A saturated solution of NaHCO<sub>3</sub> was added in order to reach a pH = 7. The two-phase solution was then extracted with dichloromethane and dried over sodium sulfate. The solution was then filtered and concentrated under rotary evaporator to reach 19.189 g of methyl oleate (yield = 91%). The product was fully characterized by GC/MS, <sup>1</sup>H-NMR and <sup>13</sup>C NMR spectroscopy. Spectra are reported in the supporting information (Figures S26–S28).

##### 4.6.2. Typical Procedure for the Epoxidation of Methyl Oleate

A 50 mL round-bottomed flask equipped with a condenser was charged with methyl oleate (**MO**, 0.50 g, 1.69 mmol), H<sub>2</sub>O<sub>2</sub> (30% w/w, 1–4 equivalent), mesitylene as internal standard (10% w/w of the substrate), the catalyst (**1–4**, 2.5–5% mol) and—where applicable H<sub>3</sub>PO<sub>4</sub> as co-catalyst (2.5% mol). The reaction was then performed at 25–75 °C, by heating the mixture under magnetic stirring (1000 rpm). Reactions were usually conducted for 4 h. At chosen intervals, an aliquot of the reaction mixture was withdrawn and analyzed by <sup>1</sup>H NMR spectroscopy to calculate conversion of MO, chemoselectivity and yield to EMO. An additional blank test was performed at 75 °C in the absence of any catalyst by setting the molar ratio H<sub>2</sub>O<sub>2</sub>:**MO** = 2.

##### 4.7. Test for the Scalability of 1-Decene Epoxidation

[N<sub>8,8,8,1</sub>]<sub>2</sub>(WO<sub>4</sub>) (5% mol respect to the substrate), hydrogen peroxide (30% w/w H<sub>2</sub>O, 2 equivalents) were charged into a round-bottomed flask equipped with a magnetic stirrer and a condenser. The mixture was stirred for 1 min and methyl oleate (**MO**, 5.021 g, 16.93 mmol) was slowly added into the flask. The mixture was heated at 75 °C and stirred at 800 rpm for 4 h. At the end of the reaction, the organic phase was separated and passed through a short plug of silica with dichloromethane as solvent in order to separate any trace of the catalyst. The product was then extracted with dichloromethane, dried over sodium sulfate and filtered. The organic phase was concentrated under reduced pressure (60 °C, 10 mbar) and epoxidized methyl oleate was obtained with a 95% yield (4.82 g, 15.42 mmol, >97% purity according to GC analysis and <sup>1</sup>H-NMR spectroscopy). The product was fully characterized by GC/MS, <sup>1</sup>H-NMR and <sup>13</sup>C NMR spectroscopy. Spectra are reported in the supporting information (Figures S29–S31).

##### 4.8. Typical Procedure for CO<sub>2</sub> Fixation Reaction into Epoxidized Methyl Oleate

Epoxidized methyl oleate (**EMO**, 0.50 g, 1.60 mmol), [N<sub>8,8,8,1</sub>]<sub>2</sub>(WO<sub>4</sub>) (5% mol), [N<sub>4,4,4,4</sub>]Br (2.5% mol) and mesitylene as internal standard (10% w/w of the substrate) were charged in a 50 mL round-bottomed flask equipped with a magnetic stirrer and closed with a perforated cap that allows the gas entrance and block the leakage of liquids. The glass reactor was placed inside a stainless-steel autoclave with an internal volume of 200 mL, equipped with a pressure gauge, a thermocouple and two valves. The autoclave was purged at room temperature by three vacuum-CO<sub>2</sub> cycles and pressurized with CO<sub>2</sub> (10–50 bar). The autoclave was then heated at 70–120 °C and the reaction was magnetically stirred (1100 rpm) for the desired period (16 h). After 16 h, the autoclave was allowed to cool, slowly vented, and opened. The final mixture was analyzed by <sup>1</sup>H NMR spectroscopy to calculate conversion of EMO, chemoselectivity to CMO and cis:trans ratio of CMO. The organic phase was finally extracted with dichloromethane, washed several times with water and dried over sodium sulfate.

This procedure was used also for the reaction conducted at atmospheric pressure of CO<sub>2</sub> (1 bar) but in this case a 50 mL two neck round-bottomed flask was used. The reagents were charged into the flask that was degassed via three vacuum-CO<sub>2</sub> cycles and a rubber reservoir containing about 2 L of CO<sub>2</sub> was connected to the reactor. The reaction vessel was sealed to prevent losses of substrates and/or CO<sub>2</sub>.

#### 4.9. Typical Procedure for the Assisted One-Pot Tandem Reaction

In a typical procedure, a 50 mL round-bottomed flask equipped with a condenser was charged with methyl oleate (MO, 2.00 g, 6.74 mmol), H<sub>2</sub>O<sub>2</sub> 30% w/w (2 equivalent 1.4 mL), mesitylene as internal standard (10% w/w of the substrate) and [N<sub>8,8,8,1</sub>]<sub>2</sub>(WO<sub>4</sub>) (5% mol). The reaction was then performed at 75 °C, by heating the mixture under magnetic stirring (1100 rpm) for 4 h. At intervals, the mixture was sampled and samples were analyzed by <sup>1</sup>H-NMR spectroscopy and GC-MS in order to follow the course of the epoxidation process. The reaction was completed after 4 h. Hence, the biphasic solution was allowed to cool at room temperature and the selected halide co-catalyst (5% mol) was added. The round-bottom glass flask was fitted inside a stainless-steel autoclave (internal volume: 200 mL) equipped with a pressure gauge, a thermocouple and two valves. The autoclave was purged at room temperature by three vacuum-CO<sub>2</sub> purge cycles and pressurized with CO<sub>2</sub> (50 bar). The autoclave was then heated at 100 °C and the reaction was magnetically stirred (1000 rpm) for 16–48 h. After the chosen time, the autoclave was allowed to cool, vented, and opened. The mixture was analyzed by <sup>1</sup>H NMR spectroscopy. At the end of the reaction, the organic phase was separated and passed through a short plug of silica with dichloromethane as solvent in order to separate any trace of the catalyst. The organic phase was then dried over sodium sulfate, filtered and concentrated under reduced pressure (60 °C, 10 mbar).

**Supplementary Materials:** The following are available online at <https://www.mdpi.com/article/10.3390/catal11121477/s1>, Figures S1–S25: NMR spectra characterization of ionic liquids, Figures S26–S34: NMR spectra and GC-MS spectra characterization of the products.

**Author Contributions:** Conceptualization, R.C. and A.P.; Methodology, R.C.; Investigation, R.C. and N.S.; Resources, A.P. and M.S.; Data Curation, R.C. and N.S.; Writing—Original Draft Preparation, R.C.; Writing—Review & Editing, M.S. and A.P.; Supervision, A.P. All authors have read and agreed to the published version of the manuscript.

**Funding:** This research received no external funding.

**Conflicts of Interest:** The authors declare no conflict of interest.

## References

1. Mac Dowell, N.; Fennell, P.S.; Shah, N.; Maitland, G.C. The role of CO<sub>2</sub> capture and utilization in mitigating climate change. *Nat. Clim. Chang.* **2017**, *7*, 243–249. [[CrossRef](#)]
2. Poliakov, M.; Leitner, W.; Streng, E.S. The twelve principles of CO<sub>2</sub> chemistry. *Faraday Discuss.* **2015**, *183*, 9–17. [[CrossRef](#)] [[PubMed](#)]
3. Selva, M.; Perosa, A.; Fiorani, G.; Cattelan, L. CO<sub>2</sub> and Organic Carbonates for the Sustainable Valorization of Renewable Compounds. In *Green Synthetic Processes and Procedures*; Royal Society of Chemistry: London, UK, 2019; pp. 319–342.
4. Aomchad, V.; Cristòfol, À.; Della Monica, F.; Limburg, B.; D’Elia, V.; Kleij, A.W.J.G.C. Recent progress in the catalytic transformation of carbon dioxide into biosourced organic carbonates. *Green Chem.* **2021**, *23*, 1077–1113. [[CrossRef](#)]
5. OECD; FAO. Oilseeds and Oilseed Products. In *OECD-FAO Agricultural Outlook 2018–2027*; OECD Publishing: Paris, France; Food and Agriculture Organization of the United Nations: Rome, Italy, 2018.
6. Ahmad, M.U. *Fatty Acids: Chemistry, Synthesis, and Applications*; Elsevier: Amsterdam, The Netherlands, 2017.
7. Karmakar, G.; Ghosh, P.; Sharma, B.K.J.L. Chemically modifying vegetable oils to prepare green lubricants. *Lubricants* **2017**, *5*, 44. [[CrossRef](#)]
8. Schäffner, B.; Blug, M.; Kruse, D.; Polyakov, M.; Köckritz, A.; Martin, A.; Rajagopalan, P.; Bentrup, U.; Brückner, A.; Jung, S. Synthesis and Application of Carbonated Fatty Acid Esters from Carbon Dioxide Including a Life Cycle Analysis. *ChemSusChem* **2014**, *7*, 1133–1139. [[CrossRef](#)] [[PubMed](#)]
9. Carré, C.; Ecochard, Y.; Caillol, S.; Avérous, L. From the synthesis of biobased cyclic carbonate to polyhydroxyurethanes: A promising route towards renewable NonIsocyanate Polyurethanes. *ChemSusChem* **2019**, *12*, 3410–3430. [[CrossRef](#)] [[PubMed](#)]

10. Danov, S.; Kazantsev, O.; Esipovich, A.; Belousov, A.; Rogozhin, A.; Kanakov, E. Recent advances in the field of selective epoxidation of vegetable oils and their derivatives: A review and perspective. *Catal. Sci. Technol.* **2017**, *7*, 3659–3675. [[CrossRef](#)]
11. Santacesaria, E.; Renken, A.; Russo, V.; Turco, R.; Tesser, R.; Di Serio, M. Biphasic model describing soybean oil epoxidation with H<sub>2</sub>O<sub>2</sub> in continuous reactors. *Ind. Eng. Chem. Res.* **2012**, *51*, 8760–8767. [[CrossRef](#)]
12. Köckritz, A.; Martin, A. Oxidation of unsaturated fatty acid derivatives and vegetable oils. *Eur. J. Lipid. Sci. Technol.* **2008**, *110*, 812–824. [[CrossRef](#)]
13. Buettner, H.; Longwitz, L.; Steinbauer, J.; Wulf, C.; Werner, T. Recent developments in the synthesis of cyclic carbonates from epoxides and CO<sub>2</sub>. In *Chemical Transformations of Carbon Dioxide*; Springer: Cham, Switzerland, 2017; pp. 89–144.
14. Tenhumberg, N.; Büttner, H.; Schäffner, B.; Kruse, D.; Blumenstein, M.; Werner, T. Cooperative catalyst system for the synthesis of oleochemical cyclic carbonates from CO<sub>2</sub> and renewables. *Green Chem.* **2016**, *18*, 3775–3788. [[CrossRef](#)]
15. Carrodeguas, L.P.; Cristòfol, À.; Fraile, J.M.; Mayoral, J.A.; Dorado, V.; Herrerías, C.I.; Kleij, A. Fatty acid based biocarbonates: Al-mediated stereoselective preparation of mono-, di- and tricarbonates under mild and solvent-less conditions. *Green Chem.* **2017**, *19*, 3535–3541. [[CrossRef](#)]
16. Langanke, J.; Greiner, L.; Leitner, W. Substrate dependent synergetic and antagonistic interaction of ammonium halide and polyoxometalate catalysts in the synthesis of cyclic carbonates from oleochemical epoxides and CO<sub>2</sub>. *Green Chem.* **2013**, *15*, 1173–1182. [[CrossRef](#)]
17. Bobbink, F.D.; Vasilyev, D.; Hulla, M.; Chamam, S.; Menoud, F.; Laurency, G.B.; Katsyuba, S.; Dyson, P.J. Intricacies of cation–anion combinations in imidazolium salt-catalyzed cycloaddition of CO<sub>2</sub> into epoxides. *ACS Catal.* **2018**, *8*, 2589–2594. [[CrossRef](#)]
18. Steinbauer, J.; Kubis, C.; Ludwig, R.; Werner, T. Mechanistic Study on the Addition of CO<sub>2</sub> to Epoxides Catalyzed by Ammonium and Phosphonium Salts: A Combined Spectroscopic and Kinetic Approach. *ACS Sust. Chem. Eng.* **2018**, *6*, 10778–10788. [[CrossRef](#)]
19. Fankhauser-Noti, A.; Fiselier, K.; Biedermann-Brem, S.; Grob, K. Assessment of epoxidized soy bean oil (ESBO) migrating into foods: Comparison with ESBO-like epoxy fatty acids in our normal diet. *Food Chem. Toxicol.* **2006**, *44*, 1279–1286. [[CrossRef](#)] [[PubMed](#)]
20. Greene, J.F.; Newman, J.W.; Williamson, K.C.; Hammock, B.D. Toxicity of epoxy fatty acids and related compounds to cells expressing human soluble epoxide hydrolase. *Chem. Res. Toxicol.* **2000**, *13*, 217–226. [[CrossRef](#)] [[PubMed](#)]
21. Calmanti, R.; Selva, M.; Perosa, A. Direct oxidative carboxylation of terminal olefins to cyclic carbonates by tungstate assisted-tandem catalysis. *Green Chem.* **2021**, *23*, 7609–7619. [[CrossRef](#)]
22. Calmanti, R.; Selva, M.; Perosa, A. J.G.C. Tandem catalysis: One-pot synthesis of cyclic organic carbonates from olefins and carbon dioxide. *Green Chem.* **2021**, *23*, 1921–1941. [[CrossRef](#)]
23. Fabris, M.; Lucchini, V.; Noè, M.; Perosa, A.; Selva, M. Ionic liquids made with dimethyl carbonate: Solvents as well as boosted basic catalysts for the Michael reaction. *Chem.-Eur. J.* **2009**, *15*, 12273–12282. [[CrossRef](#)]
24. Holbrey, J.D.; Rogers, R.D.; Shukla, S.S.; Wilfred, C.D. Optimised microwave-assisted synthesis of methylcarbonate salts: A convenient methodology to prepare intermediates for ionic liquid libraries. *Green Chem.* **2010**, *12*, 407–413. [[CrossRef](#)]
25. Busca, G. Differentiation of mono-oxo and polyoxo and of monomeric and polymeric vanadate, molybdate and tungstate species in metal oxide catalysts by IR and Raman spectroscopy. *J. Raman Spectrosc.* **2002**, *33*, 348–358. [[CrossRef](#)]
26. Calmanti, R.; Selva, M.; Perosa, A. Tungstate ionic liquids as catalysts for CO<sub>2</sub> fixation into epoxides. *Mol. Catal.* **2020**, *486*, 110854. [[CrossRef](#)]
27. Chen, Y.-G.; Gong, J.; Qu, L.-Y. Tungsten-183 nuclear magnetic resonance spectroscopy in the study of polyoxometalates. *Coord. Chem. Rev.* **2004**, *248*, 245–260. [[CrossRef](#)]
28. Ueda, T.; Kodani, K.; Ota, H.; Shiro, M.; Guo, S.-X.; Boas, J.F.; Bond, A.M. Voltammetric and Spectroscopic Studies of  $\alpha$ - and  $\beta$ -[PW<sub>12</sub>O<sub>40</sub>] 3-Polyoxometalates in Neutral and Acidic Media: Structural Characterization as Their [(n-Bu<sub>4</sub>N)<sub>3</sub>][PW<sub>12</sub>O<sub>40</sub>] Salts. *Inorg. Chem.* **2017**, *56*, 3990–4001. [[CrossRef](#)] [[PubMed](#)]
29. Poli, E.; Clacens, J.-M.; Barrault, J.; Pouilloux, Y. Solvent-free selective epoxidation of fatty esters over a tungsten-based catalyst. *Catal. Today* **2009**, *140*, 19–22. [[CrossRef](#)]
30. Clayden, J.; Greeves, N.; Warren, S.; Wothers, P. *Organic Chemistry*; Oxford University Press: Oxford, UK, 2014.
31. Poli, E.; Bion, N.; Barrault, J.; Casciato, S.; Dubois, V.; Pouilloux, Y.; Clacens, J.-M. Selective epoxidation of unsaturated fatty esters over peroxophosphotungstic catalysts (POW) under solvent free conditions: Study of the POW catalyst's mechanism. *Catal. Today* **2010**, *157*, 371–377. [[CrossRef](#)]
32. Resul, M.F.M.G.; Fernández, A.M.L.; Rehman, A.; Harvey, A.P. Development of a selective, solvent-free epoxidation of limonene using hydrogen peroxide and a tungsten-based catalyst. *React. Chem. Eng.* **2018**, *3*, 747–756. [[CrossRef](#)]
33. Wang, M.-L.; Huang, T.-H. Kinetic study of the epoxidation of 1,7-octadiene under phase-transfer-catalysis conditions. *Ind. Eng. Chem. Res.* **2004**, *43*, 675–681. [[CrossRef](#)]
34. Mizuno, N.; Yamaguchi, K.; Kamata, K. Epoxidation of olefins with hydrogen peroxide catalyzed by polyoxometalates. *Coord. Chem. Rev.* **2005**, *249*, 1944–1956. [[CrossRef](#)]
35. Pai, Z.P.; Khlebnikova, T.B.; Mattsat, Y.V.; Parmon, V.N. Catalytic oxidation of fatty acids. I. Epoxidation of unsaturated fatty acids. *React. Kinet. Catal. Lett.* **2009**, *98*, 1–8. [[CrossRef](#)]

36. Musik, M.; Janus, E.; Pelech, R.; Sałaciński, Ł. Effective Epoxidation of Fatty Acid Methyl Esters with Hydrogen Peroxide by the Catalytic System  $H_3PW_{12}O_{40}$ /Quaternary Phosphonium Salts. *Catalysts* **2021**, *11*, 1058. [[CrossRef](#)]
37. Deferm, C.; Van den Bossche, A.; Luyten, J.; Oosterhof, H.; Fransaeer, J.; Binnemans, K. Thermal stability of trihexyl (tetradecyl) phosphonium chloride. *Phys. Chem. Chem. Phys.* **2018**, *20*, 2444–2456. [[CrossRef](#)]
38. Galvan, M.; Selva, M.; Perosa, A.; Noè, M. Toward the Design of Halide-and Metal-Free Ionic-Liquid Catalysts for the Cycloaddition of  $CO_2$  to Epoxides. *Asian J. Org. Chem.* **2014**, *3*, 504–513. [[CrossRef](#)]
39. Blundell, R.K.; Licence, P. Quaternary ammonium and phosphonium based ionic liquids: A comparison of common anions. *Phys. Chem. Chem. Phys.* **2014**, *16*, 15278–15288. [[CrossRef](#)] [[PubMed](#)]
40. Carvalho, P.J.; Ventura, S.P.; Batista, M.L.; Schröder, B.; Gonçalves, F.; Esperança, J.; Mutelet, F.; Coutinho, J.A. Understanding the impact of the central atom on the ionic liquid behavior: Phosphonium vs ammonium cations. *J. Chem. Phys.* **2014**, *140*, 064505. [[CrossRef](#)] [[PubMed](#)]
41. Doll, K.M.; Erhan, S.Z. The improved synthesis of carbonated soybean oil using supercritical carbon dioxide at a reduced reaction time. *Green Chem.* **2005**, *7*, 849–854. [[CrossRef](#)]
42. Natongchai, W.; Pornpraprom, S.; D’Elia, V. Synthesis of Bio-Based Cyclic Carbonates Using a Bio-Based Hydrogen Bond Donor: Application of Ascorbic Acid to the Cycloaddition of  $CO_2$  to Oleochemicals. *Asian J. Org. Chem.* **2020**, *9*, 801–810. [[CrossRef](#)]
43. Cai, T.; Liu, J.; Cao, H.; Cui, C. Synthesis of bio-based cyclic carbonate from vegetable oil methyl ester by  $CO_2$  fixation with acid-base pair MOFs. *Ind. Crops Prod.* **2020**, *145*, 112155. [[CrossRef](#)]
44. Kimura, T.; Kamata, K.; Mizuno, N. A bifunctional tungstate catalyst for chemical fixation of  $CO_2$  at atmospheric pressure. *Angew. Chem. Int. Ed.* **2012**, *51*, 6700–6703. [[CrossRef](#)]
45. Sels, B.; De Vos, D.; Buntinx, M.; Pierard, F.; Kirsch-De Mesmaeker, A.; Jacobs, P. Layered double hydroxides exchanged with tungstate as biomimetic catalysts for mild oxidative bromination. *Nature* **1999**, *400*, 855–857. [[CrossRef](#)]
46. Podgoršek, A.; Zupan, M.; Iskra, J. Oxidative halogenation with “green” oxidants: Oxygen and hydrogen peroxide. *Angew. Chem. Int. Ed.* **2009**, *48*, 8424–8450. [[CrossRef](#)] [[PubMed](#)]
47. Liu, W.; Lu, G.; Xiao, B.; Xie, C. Potassium iodide–polyethylene glycol catalyzed cycloaddition reaction of epoxidized soybean oil fatty acid methyl esters with  $CO_2$ . *RSC Adv.* **2018**, *8*, 30860–30867. [[CrossRef](#)]
48. Longwitz, L.; Steinbauer, J.; Spannenberg, A.; Werner, T. Calcium-based catalytic system for the synthesis of bio-derived cyclic carbonates under mild conditions. *ACS Catal.* **2018**, *8*, 665–672. [[CrossRef](#)]
49. Alassmy, Y.A.; Pescarmona, P.P. The Role of Water Revisited and Enhanced: A Sustainable Catalytic System for the Conversion of  $CO_2$  into Cyclic Carbonates under Mild Conditions. *ChemSusChem* **2019**, *12*, 3856–3863. [[CrossRef](#)] [[PubMed](#)]